

NORTHWEST AFRICA 14091: A NEW STANNERN-GROUP EUCRITE FROM ALGERIA. R. Kared¹, A. Seddiki¹, B. N. Moine², R.C. Greenwood³, J. Y. Cottin⁴ and I.A. Franchi³, ¹Laboratoire GEOREN, Univ. Oran 2-MBA-Oran, Algeria (ratibakared@yahoo.com); ²Université Clermont Auvergne, CNRS, IRD, OPGC, Laboratoire Magmas et Volcans, F-63000 Clermont-Ferrand, France; ³Planetary and Space Sciences, Department of Physical Sciences, The Open University, Walton Hall, Milton Keynes MK7 6AA, UK; ⁴Laboratoire LGL-TPE UMR CNRS 5276 (CNRS, ENS, Université Lyon1, UJM-Saint-Etienne) F-42023, Saint-Etienne Cedex 02, France.

Introduction: The HEDs (howardites, eucrites, and diogenites) are a clan of meteorites that originate from the asteroid (4) Vesta [1-2]. The eucrites are basalts and gabbros composed mainly of plagioclase and pyroxenes [3]. Based on their composition, there are three divisions in Basaltic eucrites: main group, Nuevo Laredo-trend and Stannern-trend [4]. The Stannern trend eucrites, which is the least dominant eucrite, have Mg# like the main group eucrites, but with specific enrichments in incompatible trace elements [5]. In this study, we identify and examine eucrite NWA 14091, a new member of this scarce trend, discovered in the Sahara of Southwest Algeria.

Methods: petrographic observations and major analyses were made on polished section (of about 1.5 cm²). Backscatter electron (BSE) maps were performed with scanning electron microscope with an accelerating voltage of 15 kV. Major and minor element concentrations were determined by electron microprobe analysis (CAMECA S×100, 15 kV, 20 nA), trace element analyses by ICPMS solution (Agilent 7500 CX) at Magmas and Volcanoes laboratory (LMV) – Clermont-Ferrand – France. Oxygen isotopes analysis was undertaken out at the Open University using an infrared laser-assisted fluorination system [6-7].

Petrography: NWA 14091 is a 37 gram eucrite. It is a monomict basaltic eucritic breccia, with a partially preserved fusion crust. The sawn surfaces display several clasts and clastic matrix (Fig. 1). The sample shows fracturing and granulation resulting from the shock effects. The sample presents clasts with different textures with same lithology. The first is sub-ophitic represented by large grains (~ 600 µm) of poikilitic pyroxene including large plagioclase (100 to 800 µm) as shown in the figure (Fig. 2A). The second one is ophitic texture represented by small grains (100 µm) and finally, the last one is very fine-grained texture including some large pyroxene phenocryst (200 µm) (Fig. 2B).

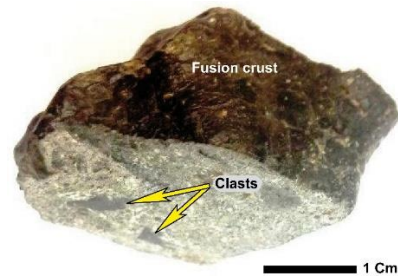


Figure 1: Photograph of NWA 14091 showing brecciated nature of the sample with a partial black fusion crust.

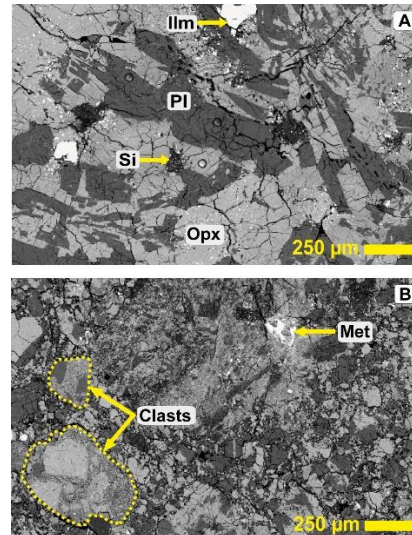


Figure 2: Backscattered electron images (BSE) of characteristic mineral assemblages and textures within NWA 14091. **A:** Sub-ophitic texture; **B:** Overview of the brecciated area, showing a fine-grained texture in which there are large grains of pyroxene. *Abbreviations used:* Opx = Orthopyroxene; Pl = Plagioclase; Si = Silica; Ilm = Ilmenite and Met = Fe-metal.

Pyroxenes occur as subhedral grains in ophitic clasts (500 µm to 1 mm) while the grains of the matrix are mostly fractured and variable in size that can be up to 200 µm in longest dimension. Most plagioclases are present as subhedral grains in the sub-ophitic areas (100 to 800 µm). Ilmenite grains are subhedral (100 to 250 µm) associated with plagioclase and pyroxene grains or in the matrix. Chromite occurs as small subhedral grains (<100 µm) within or in contact with pyroxene. Troilite and Fe-metal grains are observed as

accessory phases, they are typically <80 in size. Silica is observed and it is associated with small grains of troilite in the most brecciated areas.

Mineral compositions and Oxygen isotopes analyses: Electron microprobe analyses show wide variation in phase compositions between magmatic and high temperature metamorphic compositions. Pyroxene compositions vary in the range of $Wo_{5.47-28.01} En_{33.35-40.3} Fs_{38.65-55.21}$ for pigeonite, $Wo_{2-4.39} En_{38.74-44.91} Fs_{53.09-56.95}$ for low calcium pyroxene and $Wo_{21.01-42.07} En_{32.21-36.88} Fs_{25.71-42.55}$ for high calcium pyroxene (Fig. 3). All Fe/Mn ratios lie between 25.8 and 36.44. The plagioclases of NWA 14091 are mainly bytownites $An_{72.24-90.91} Or_{0.25-2.8}$. The La and Sc concentrations of the whole rock are respectively 4.5 $\mu\text{g/g}$ and 27.2 $\mu\text{g/g}$. The oxygen isotopic composition obtained on two aliquots of NWA 14091 is $\delta^{17}\text{O} = 1.807 \pm 0.008 \text{ ‰}$ (2σ); $\delta^{18}\text{O} = 3.889 \pm 0.004 \text{ ‰}$ (2σ); $\Delta^{17}\text{O} = -0.231 \pm 0.026 \text{ ‰}$ (2σ).

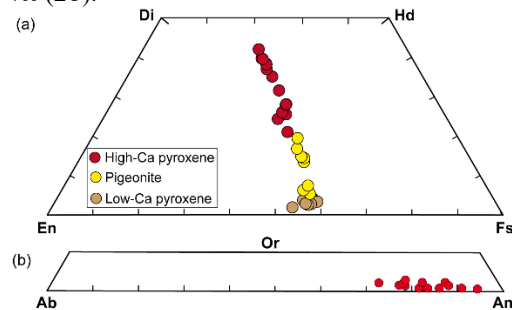


Figure 3: Major element compositions in (a) pyroxene and (b) plagioclase from NWA 14091.

Discussion : Trace element concentration and FeO/MgO ratio (Figure 4) show that NWA14091 is linked to the Stannern trend, along with the data for other eucrites of literature compiled by [5]. We suggest that NWA 14091 is classified as a new Stannern group eucrite. This trend is suggested being among the youngest eucrites to have erupted at the surface of 4Vesta [8]. According to the classification of [9], NWA 14091 has the metamorphic characteristics of type 2-4 eucrites. Hence, we agree with [5] that The Stannern trend eucrites are among some of the least metamorphosed in the range types 1–4. Thus, the metamorphism of this eucrite could be an impact metamorphism related to the shock. The crystals present in the clastic matrix are essentially breccias, but some of them present high resistances (Fig. 2). This could be explained by the fact that this eucrite has undergone heterogeneous shock effects as previously suggested [10].

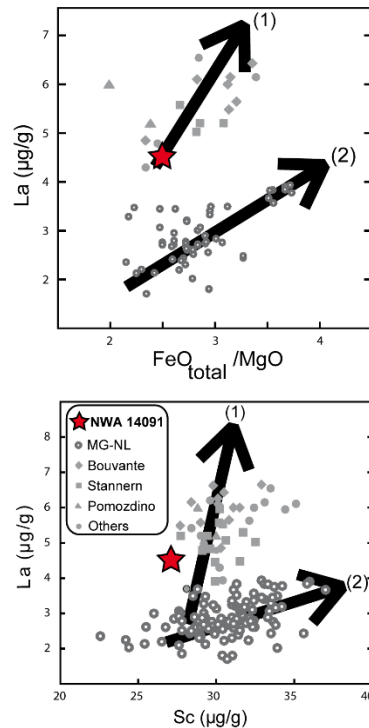


Figure 4: Plots of La vs. $\text{FeO}_{\text{total}}/\text{MgO}$ and La vs. Sc for NWA 14091. (1) Stannern trend; (2) Main group, Nuevo Laredo-trend. These two plots are compared with literature data taken from [5].

References: [1] McCord T. B. et al. (1970) *Science* 168, 1445–1447. [2] McSween, H. Y. et al. (2013) *Journal of Geophysical Research* 118, 335–346. [3] Mayne R. G. et al. (2010) *Meteoritics & Planetary Science* 7, 1074–1092. [4] Gardner K. G. and Mittlefehldt D.W. (2004) 33rd *Lunar Planet. Sci. XXXV* # 1349.. [5] Barrat J. A. et al. (2007) *Geochimica et Cosmochimica Acta* 16, 4108–4124. [6] Greenwood R. C. et al. (2016) *Chemie der Erde* 77, 1–43. [7] Miller M. F. et al. (1999) *Rapid Communications in Mass Spectrometry* 13, 1211–1217. [8] Warren P. H. and Kallemeyn G. W. (2001) *Lunar Planet. Sci.* 32 #2114. [9] Takeda H. and Graham A. L. (1991) 26, 129–134. [10] Yamaguchi A. et al. (2006) *Meteoritics & Planetary Science*. 41, 863–874.